Steady State Tearing in Thin Aluminium Sheets under Uniaxial Tension

V.P. Naumenko and Yu.D. Skrypnyk
Leading scientist and senior scientist, G.S. Pisarenko Institute for Problem of Strength,
2 Timiriazevskaya str., Kyiv 01014, Ukraine, E-mail: v.p.naumenko@ipp.kiev.ua

Abstract

Experimental data on the Steady State Tearing (SST) in middle-cracked tension specimens of different geometry are examined with the use of global parameters characterizing the mechanical behavior of a "moving crack tip" embedded into a fully developed "moving neck". They both spread across the ligament under different levels of constraint produced by varying the in-plane geometry of specimens. The proposed criteria of attaining the SST stage are expressed in terms of averaged quantities, which enable accounting for the plasticity and damage effects immediately from test records.

Introduction

Thin-wall structures made of ductile metals are encountered in many applications in aerospace, mechanical, civil and ocean engineering. The loading conditions in such structures tend to be uniaxial or biaxial tension. When it comes to the case of a straight-through crack slowly growing under uniaxial tension, the fracture process is accompanied by the development of low-constrained flow fields. In center-cracked specimens made of thin-sheet metals, the in-plane constraint depends on geometry and size of its Problem Domain (PD), initial crack length and amount of crack advance, restraints imposed on the boundaries of the PD, the material deformation behavior, prior loading history, and the magnitude of applied load.

The long-term aim of this, as well as previous, studies of Naumenko *et al.* [1-9] is to develop a Transferring Law (TL), i.e., a common function for the test data on plane stress crack growth in a simple specimen of relatively small size and in a large-scale component of complicated geometry. An easy-to-use TL should allow simple correlation of the data for the specimen and the component with a minimum number of parameters. That is why our attention is focused on the SST stage described in terms of the tensile load, displacements of the extreme points on a center-cracked plate, and crack extension increment. The extreme points (*m* and *n* in Fig.1) on the inner boundary, i.e., on the crack surfaces, are shown together with the corresponding extreme points *M* and *N* on the outer boundaries of the PDs in question. The objective of this work is to check experimentally whether it is possible, using only global fracture parameters, to assess the SST crack growth under uncontained yielding in differently constrained specimens. In general, our approach to the characterization of plane stress tearing [1-9] may be thought of as an alternative to the novel approaches developed by Chabanet *et al.* [10], Sumpter [11] and Pardoen *et al.* [12]. They employ (i) the Gurson-Tvergaard-Needleman and the cohesive zone models for predicting the crack growth resistance of aluminium sheets [10], (ii) a new fracture analysis based on the energy dissipation rate *D* [11], and (iii) the model allowing independent evaluation of the work of necking and the work of fracture [12].

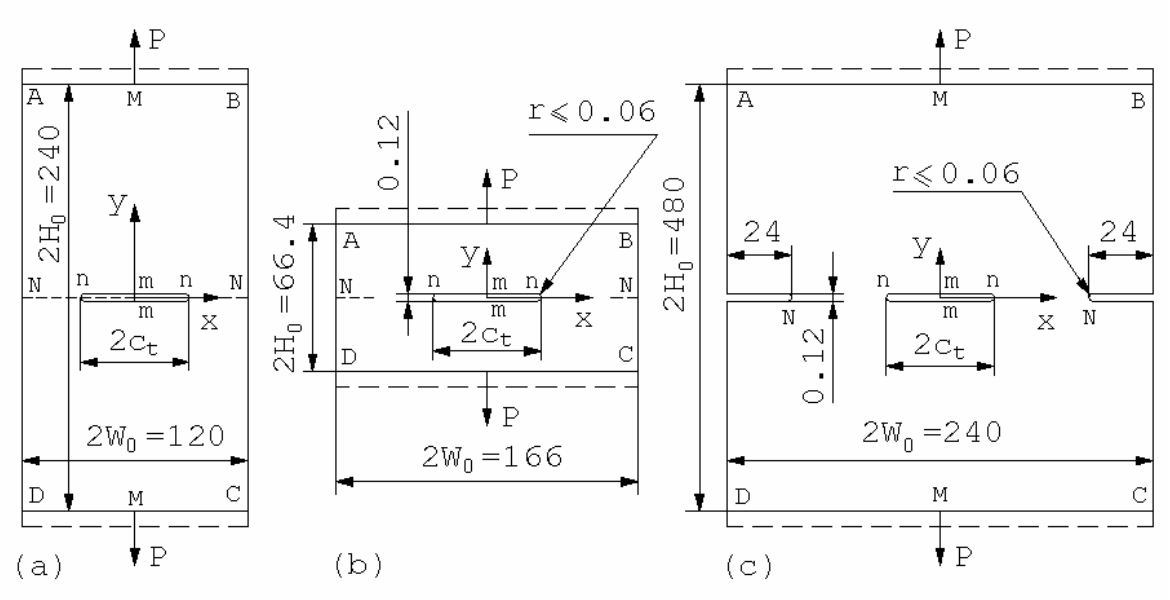

FIGURE 1. A center crack in tension-dominant problem domain ABCD designated as (a) LM(T)-2.0, (b) HM(T)-0.4 and (c) MDEN(T) specimens. All sizes in mm.

Specimens and Testing

The test material is a high-strength low-hardening aluminium alloy 1163 AT having the form of 1.05 mm thick sheets. Its chemical composition and mechanical properties are nearly identical to those of AL 2024-T3. The tensile properties under ambient conditions are as follows: the elastic modulus E = 73 GPa, the Poisson's ratio ν = 0.32, the 0.2% offset yield stress σ_Y = 334 MPa, and the ultimate strength σ_u = 446 MPa. Crack growth tests were performed on specimens containing low-stress fatigue precracks at the tips of starting slots of length $2c_t$ (Figs 1a and 1c). Two extremely different initial stress raisers were used in tests of highly-constrained specimens shown in Fig. 1b. One of them introduces the minimum and the other the maximum levels of initial damage. By convention, a starting slot of height $2r \leq 0.12$ mm with the tips curvature $r \leq 0.06$ mm is taken as a damage-free stress raiser. A tearing precrack represents the other extreme of the loading history for which crack-tip blunting, residual stress-strain fields, local neck and shear lips are considered to be fully developed. In tear precracking, the level of the net-section stress σ_N was above the yield stress σ_Y of the material.

Buckling restraints were used in the tests of each specimen under investigation. In the course of crosshead-displacement controlled tests, the specimens were loaded incrementally, allowing time to measure load-point displacement, Crack Mouth Opening Displacement (CMOD), and crack length and enabling us to make a close-up photograph of the near-crack-tip profile. During the tests of the MDEN(T) specimens (Fig. 1c), four diagrams were recorded simultaneously, namely: load P versus displacement $2v_m$ of the extreme points m , load P versus displacement $2v_M$ of the extreme points M, load P versus displacement $2u_n$ of the initial crack tip, and load P versus displacement $2u_N$ of the extreme points N. It is pertinent to mention that the presence of two edge notches in this specimen concentrate all the thinning, damage, and cracking inside two localized necks spreading initially from points n towards points N.

Critical Events and Fracture Parameters

To establish the critical states of differently constrained specimens in a unified manner, we use a new macrointerpretation of the test records, which was introduced earlier in [7-9] and is shown in Figs 2 and 3. Two critical points "*e*" and "*s*" designate the lower and upper limits of the instability event "*c*". They can be derived directly from raw experimental data presented in the form of the load *P* versus half-crack length *c* diagram. The focus is on the softening portion of the diagram (Figs 2a and 3a) reflecting the highest load-carrying capacity of the specimen. The two-point definition of the critical state *"c"* is based on presentation of the test data by linear segments, which follows from the notion of the SST adopted in [6,7].

The SST is treated as the process of omnidirectional extension of the center crack cavity, which is represented in the analysis by a stress-free cavity of an equivalent elliptic hole [1]. One of the main conditions for an adequate macroscopic description of the fracture process is the equality of the spacings 2s and 2c between the extreme points *m* and *n* for the hole to those between the same points for the actual crack. It is assumed that the geometry-independent resistance to slow-stable crack growth is only recovered under the following SST conditions. The crack is driven forward at a constant level of the net-section stress σ_{Ns} and the increments $2\Delta s$ in the Crack Mouth Opening Spacing (CMOS) are in direct proportion to the increments $2\Delta c$ in the crack length $2c$. The CMOS value is given by $2s = 2(s_u + v_m)$, where $2s_u$ is its unrecoverable component.

To determine the s_u value, one need to initiate cracking from the tips of the initial stress raiser with monotonically and slowly increasing load point displacement $2v_M$. After a sufficient amount of the post-peak crack growth ($\Delta c > \Delta c_s$ in Figs. 2a and 3a), the fracture process must be interrupted at the point "*a*" by monotonic unloading. Further, the crack extension resistance curve expressed in terms of the CMOD is used for evaluating the Crack Mouth Opening Angle (CMOA). Its values for unloaded specimens are shown in Fig.4. It can be seen that the angle α_{su} values for the initial stress raisers of different

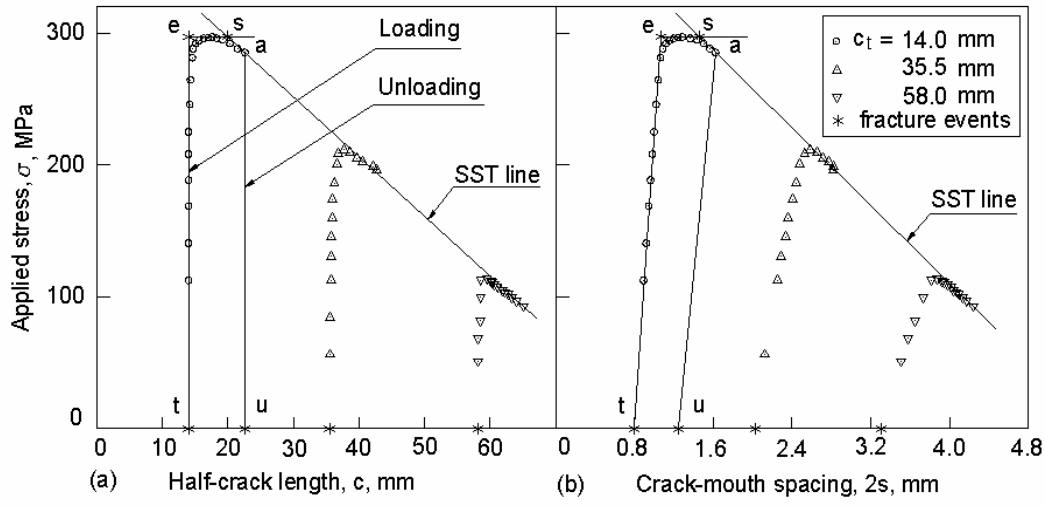

FIGURE 2. Sequences of test records and fracture events for three HM(T)-0.4 specimens with tear precracks of the lengths 28, 71 and 116 mm: the initial "*t*" and unloaded "*u*" states are shown together with the critical events "*e*", "*s*" and "*a*" for c_t = 14 mm.

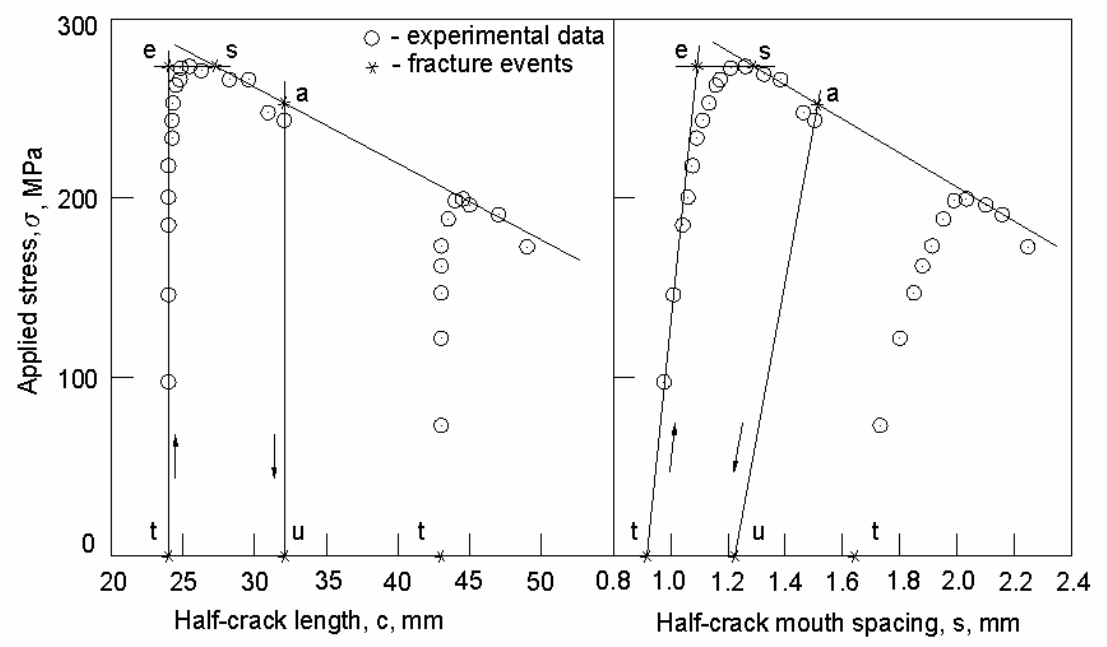

FIGURE 3. Sequences of test records and fracture events for two MDEN(T) specimens.

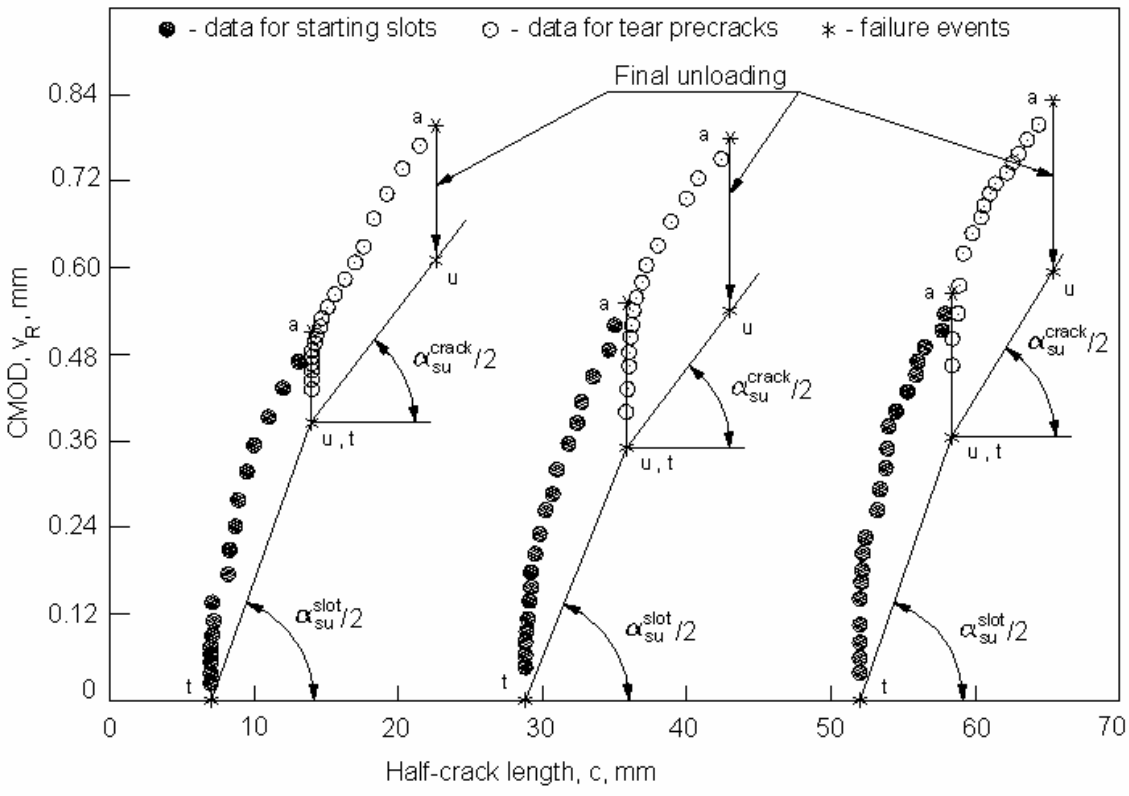

FIGURE 4. Sequences of R-curves for three HM(T)-0.4 specimens, which contained starting slots of different lengths that were transformed into tear precracks by the termination of stable crack growth due to complete unloading at the point *u, t*.

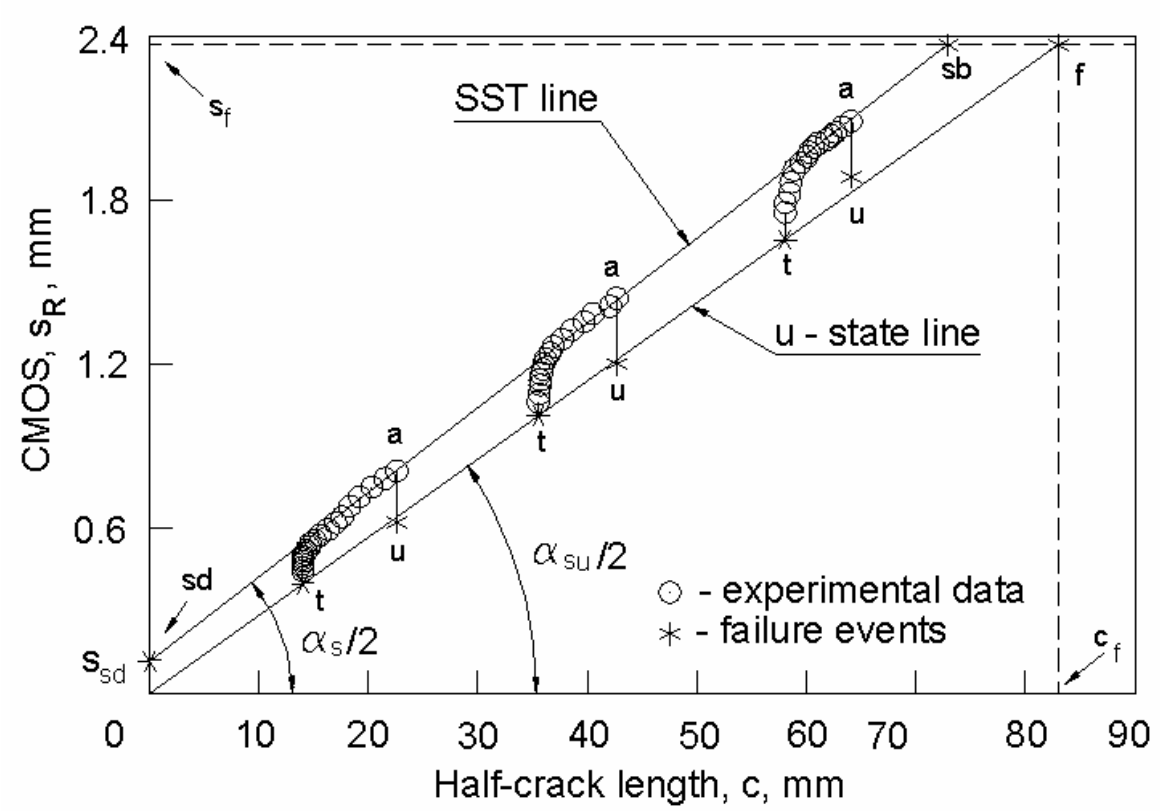

FIGURE 5. Sequences of s_R-curves for three HM(T)-0.4 specimens with tear precracks, which follow from the graphic displays of the test data in Figs. 2 and 4.

length are nearly equal and, at the same time, they are distinctly different for the starting slots and the tear precracks.

The v_R-curves for tear precracks in Fig. 4 are represented in Fig.5 as the s_R-curves. Taken together with the test data given in Fig. 2, they allow us to introduce a new definition of the term Naturally-Forming Crack (NFC). The NFC denotes an imaginary tear crack that is nucleated near the center point of a thin rectangular plate. The CMOS value s_{sd} (see Figs 5 and 6) is the main dimension of the NFC in a given PD under prescribed boundary conditions. This simplified treatment of the SST is used for characterizing the crack extension resistance in terms of the total angle α_s, specific work of fracture A_s, and Crack Volume Ratio (CVR), which is a new fracture parameter. They are defined as follows:

$$\alpha_s = \alpha_{su} + \alpha_{st} = 2 \cdot \tan^{-1}\left(\frac{s_f - s_{sd}}{c_f}\right), \tag{1}$$

$$\alpha_{su} = 2 \cdot \tan^{-1}\left(\frac{s_f}{c_f}\right), \tag{2}$$

$$A_s = A_{su} + A_{st} = \left(2W_N - c_{s0} - c_{sb}\right) \cdot \sigma_{NS} \cdot tg\frac{\alpha_s}{2}, \tag{3}$$

$$A_{su} = \left(2W_N - c_{s0} - c_{sb}\right) \cdot \sigma_{NS} \cdot tg\frac{\alpha_{su}}{2}, \tag{4}$$

$$V_{et} = C_e \cdot \frac{\sigma_t + \sigma_e}{E} + \frac{2h_{et}}{\pi\sqrt{\rho_0 c_t}}, \tag{5}$$

$$V_{st} = C_s \cdot \frac{\sigma_u + \sigma_s}{E} + \frac{2h_{st}}{\pi\sqrt{\rho_0 c_u}}. \tag{6}$$

Here, $2s_f$ and $2c_f$ are the CMOS and the crack length at the instant "*f*" of complete loss of load-carrying capability when $c = c_f \approx W_N$ (see Figs 5 and 6), W_N is the half-width of the ligament, B_0 is the specimen thickness, σ_t and σ_u are the internal stresses related to the initial state "*t*" and the unloaded state "*u*", respectively, (see Figs 2 and 3), and h_{et} and h_{st} are the increments in the height h of the active damage zone due to external loading. The radius $\rho_0 = 0.262$ mm is treated as the characteristic of an actual crack in a given material of a given thickness. The stress concentration factor C_e and C_s takes the form

$$C = F_v\left(\frac{L}{W_N}\right) \cdot \left(1 + 2 \cdot \sqrt{\frac{c_t}{\rho_0}} - k\right), \tag{7}$$

where L is the effective size of an equivavent elliptic hole, $L = l + 0.5 \cdot (1-k) \cdot \sqrt{\rho_0 l}$, l is the length of this hole, F_v is the non-dimensional function of the crack border compliance, k is the ratio of the loads applied along and across the crack line. The procedures used for estimating the values of ρ_0, σ_t, σ_u, V_{et}, V_{st}, and A_s are outlined in [6-9].

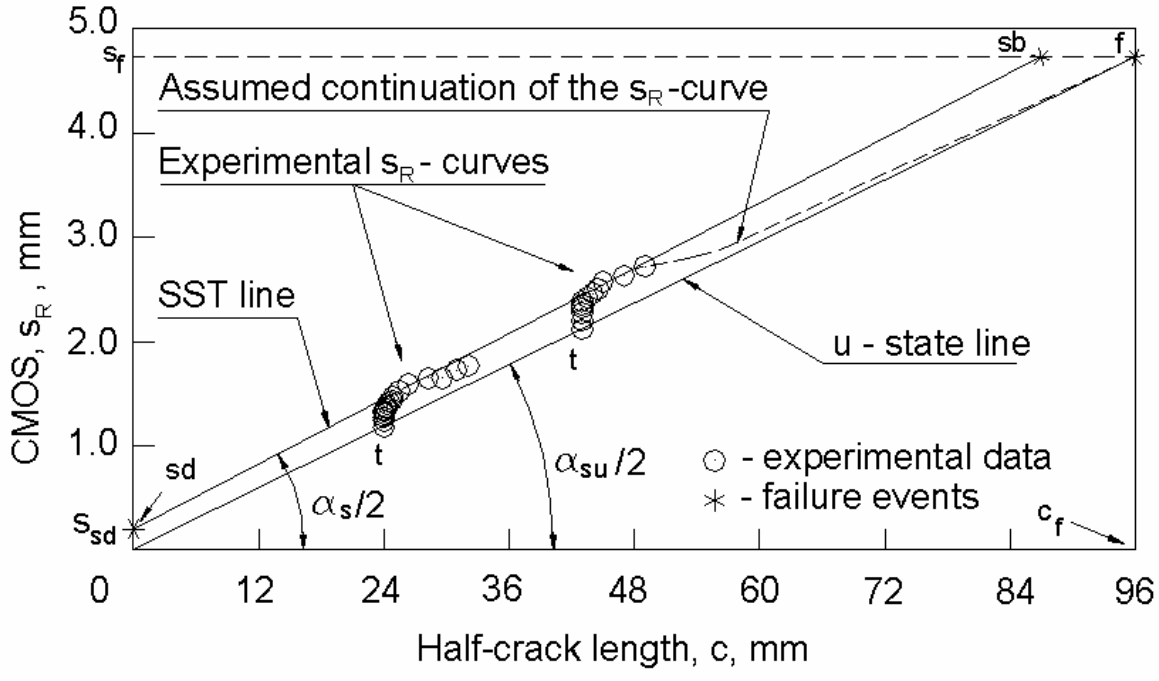

FIGURE 6. Sequences of s_R-curves following from the test data for two MDEN(T) specimens presented in Fig 3.

TABLE 1. Characteristics of the SST crack growth in AL 1163 AT specimens.

Specimen code	Initial stress raiser: type and length, $2c_t$, mm	$\frac{\alpha_{su}}{\alpha_{st}}$, degree	$\frac{h_{et}}{h_{st}}$, mm	$\frac{V_{et}}{V_{st}}$	$\frac{A_{su}}{A_{st}}$, MJ/m^2
LM(T)-2.0	Fatigue precracks 12.4 – 48.3	5.336 [a] / 0.581	0.1442 [b] / 0.1673	0.1553 [b] / 0.1698	0.976 [a] / 0.106
HM(T)-0.4	Starting slots 14 – 104	6.548 [a] / 0.218	…	…	1.603 [a] / 0.053
	Tear precracks 28 -116	3.265 [a] / 0.266	…	...	0.754 [a] / 0.061
MDEN(T)	Two fatigue precracks 48 and 86	5.633 [a] / 0.324	0.1836 [b] / 0.2198	0.1937 [b] / 0.2031	1.573 [a] / 0.091

[a] The values above and below the line are related to the states "*u*" and "*s*", respectively.
[b] A similar relation, but to the states "*e*" and "*s*", respectively.

Results and Discussion

All fracture parameters presented in Table 1 are based on the characterization of the entire crack profile in terms of the (P - v_m - Δc) data. We believe that an engineering criterion for assessing the SST crack growth should be reasonably independent, at least, of the PD geometry, its size, and the length of an initial stress raiser. As can be seen from Table 1, there is no sufficiently general criterion of attaining the SST stage. Of those presented in Table 1, the active damage zone characteristics, i.e., α_{st} and A_{st}, are preferable because of relatively weak sensitivity to prior loading history. Uncoupled from the remote plasticity components α_{su} and A_{su}, they may be used in engineering assessment of the critical state of a growing crack under uncontained yielding. The values α_{st} and A_{st} determined on the highly-constrained HM(T)-04 specimens can be treated as the material fracture properties unaffected by the changes in the initial crack length and the geometry and size of a center-cracked specimen. Under such conditions, equations (1-4) could provide conservative predictions of the failure load P_s, crack border spacing $2s_s$, and stable crack extension Δc_s for uniaxially loaded center-cracked plates and shells made of thin-sheet ductile materials.

During the SST crack growth the load P is directly related to the changes in the geometric parameters characterizing global deformation of the inner and outer boundaries of a center-cracked PD. These parameters are called the crack distortion ratio d_{cs} and the boundary distortion ratio d_{bs}, respectively, and given by

$$d_{cs} = \frac{u_n}{v_m} \cdot \frac{s_f}{c_f} \qquad \text{and} \qquad d_{bs} = \frac{u_N}{v_M} \cdot \frac{H_{Mf}}{W_{Nf}} \ . \tag{8}$$

They may be incorporated in fracture analysis as new in-plane constraint parameters. Our measurements of the displacements u_n, u_N , v_m and v_M demonstrate that a decrease in the spacing $2H_M$ between the rigidly clamped boundaries of the PD with a fixed size of $2W_N$

causes the constraint level to rise. This level is determined by the degree of proximity to the conditions of the plane strain necking, i.e., there are no displacements of the outer PD boundaries along the crack line ($W_{Nf} = W_0$). The HM(T)-0.4 specimen geometry provides higher in-plane constraint than the more complicated one of the MDEN(T) specimen.

Conclusions

1. The global characteristics α_{st} and A_{st} make it possible to assess simply and safely the beginning of the SST crack growth stage under uncontained yielding.
2. There are clear indications that among tension-dominant crack geometries the one of HM(T)-0.4 specimens is the most suitable for standard crack extension tests of thin-sheet metals.

Acknowledgements

We are grateful to the Science and Technology Center in Ukraine and the European Union for providing financial support of this presentation through the STCU project No. 2212.

References

1. Naumenko, V.P., In *Proceedings of the Eleven European Conference on Fracture*, edited by M.M. Brown, E.R. de los Rios, K.J. Miller, Sheffield, 1998, 1083-1088.
2. Naumenko, V. P., Kolednik, O., O'Dowd, N. P., Volkov, G. S., and Semenets, A. I., In *Proceedings of the Twelfth European Conference on Fracture,* edited by M. W. Brown, E. R. de los Rois, and K. J. Miller, Vol. 2, 1998, 631-636.
3. Naumenko, V. P., Kolednik, O., O'Dowd, N. P. and Volkov, G. S., In *Proceedings of the International Conference LAMSC*, edited by V. T. Troshchenko, Vol.1, 2000, Logos, Kiev, Ukraine, 299-304.
4. Naumenko, V. P., Volkov, G. S., and Atkins, A. G., In *Proceedings of the Thirteenth European Conference on Fracture,* San Sebastian, 2000, 1A.34.8 pages.
5. Naumenko, V.P., Volkov, G.S., and Atkins, A.G., In *Proceedings of the Sixth International Conference on Biaxial/Multiaxial Fatigue and Fracture,* edited by M.M. de Freitas, Lisboa, 2001, 975-982.
6. Naumenko, V.P., In *Proceedings of the Fourteenth European Conference on Fracture*, edited by A. Neimitz, I.V. Rokach, D. Kocanda, K. Golos, EMAS, Sheffield, 2002, Vol.2., 543-550.
7. Naumenko, V.P., Volkov, G.S., In *Proceedings of the Sixth International Conference* on Engng. Struct. Integrity Assessment, Manchester, 2002, 8 p.
8. Naumenko, V.P., Volkov, G.S., In *Proceedings of the Second ASTM-ESIS Conference on Fatigue and Fracture Mechanics, ASTM STP1461*, edited by S.R.Daniewicz, J.C.Newman and K.-H.Schwalbe, West Conshohocken, PA, 2003.
9. Naumenko, V.P. and Atkins, A.G., In *Proceedings of the Seventh International Conference on Biaxial/Multiaxial Fatigue and Fracture,*Berlin, 2004, 6 pages.
10. Chabanet, O., Steglich, D., Besson, J., Heitmann, V., Hellmann, D., Brocks, W., *Computational Materials Science*, 26, 2003, 1-12.
11. Sumpter, J.D.G., *Engineering Fracture Mechanics*, 71, 2004, 17-37.
12. Pardoen, T., Hachez, F., Marchioni, B., Blyth, P.H., Atkins, A.G., *J. Mech. Phys. Solids*, 52, 2004, 423-452.